

# Modelling of Time-varying Rough Sea Surface Ghosts and Source Deghosting by Integral Inversion

E. Cecconello\* (Petroleum Geo-Services / UiO), E.G. Asgedom (Petroleum Geo-Services), O.C. Orji (Petroleum Geo-Services), W. Söllner (Petroleum Geo-Services)

## Summary

---

A major impediment to the full understanding of the data acquired in marine seismic is the restricting assumption of a flat and stationary sea surface used in certain pre-processing tools. A first step towards removing this assumption is to accurately account for the sea state (time varying free surface) in the deghosting process. On the receiver side, this is handled properly by using dual-sensor streamer. In this work, we present an integral approach to model the source side ghost effects from time-varying rough sea surfaces and show that the interaction with time-varying sea surfaces affect the subsurface reflections and may have a significant impact on seismic repeatability. We then continue with a theoretical derivation where we develop deghosting operator based on an integral inversion of the modeling operator. This formulation for source deghosting can account for the time-variation of rough sea surfaces.

## Introduction

Sea surface interaction, if not properly handled during processing, penalizes the resolution of the seismic data. The delayed signals coming from the reflection at the sea surface will interfere destructively or constructively with the subsurface reflections. Conventional data processing techniques that handle sea surface ghosts are generally limited to the flat sea surface assumption (Fokkema and van den Berg (1993); Amundsen (2001)). In recent years, some of these techniques have been extended to account for the variable sea surface profile (Laws and Kragh (2002); Orji et al. (2012); Asgedom et al. (2016)). Nevertheless, the algorithms still neglect the time dependency of the sea surface. With the advent of the dual sensor acquisition concept, which enables the separation of the acquired wavefield into its upgoing and downgoing components (Tenghamn et al. (2007)), this assumption can be relaxed on the receiver side.

The first step for accurate removal of sea surface ghosts starts with a thorough investigation of rough weather ghost effects by forward modelling. Ceconello et al. (2016) present an integral approach to model the receiver side ghost effects from time-varying rough sea surfaces. In this paper, we follow the same method to model source side ghost effects. Finally, we present an integral inversion method for source deghosting that handles time-varying sea surfaces.

## Methodology

**Ghost modelling:** The interaction of seismic wavefields with a stationary rough sea surface can be modeled based on the reciprocity theorem (Fokkema and van den Berg (1993)). In the case of a time-varying rough sea surface, the main steps for modeling the receiver-side ghost have been presented in Ceconello et al. (2016). In this work on the source-side, starting with the time-dependent version of acoustic reciprocity, we couple the three states A, B and C (cf. Fig 1). First, combining the pressure wavefield from state A with the pressure gradient from state B, we obtain the scattered pressure wavefield from the sea surface. Subsequently, the gradient of this scattered wavefield is coupled with the subsurface reflectivity from state C at the separation level to model the upgoing (at both source and receiver sides) pressure wavefield  $p_s^{-,-}$ , i.e. the source ghost:

$$p_s^{-,-}(\mathbf{x}_r, t - t_r - t_s; \mathbf{x}_s, 0) = -2 \int_{-\infty}^{+\infty} \int_{S_0} [p^{C-,+}(\mathbf{x}_r, t - t_r - t_1; \mathbf{x}_{sep}, 0) \times \int_{-\infty}^{+\infty} \int_{S_f(t)|_{t=t_2+t_r^A}} [\nabla p^B(\mathbf{x}_{sep}, t_1 - t_2; \mathbf{x}_{surf}, 0) \nabla^{S_f} p^A(\mathbf{x}_{surf}, t_2; \mathbf{x}_s, t_s)] \cdot \mathbf{n}_f dS_f(t)|_{t=t_2+t_r^A} dt_2] \cdot \mathbf{n}_d S_0 dt_1 \quad (1)$$

In state A, the pressure gradient  $\nabla^{S_f} p^A$ , generated at the source  $\mathbf{x}_s$  at time  $t_s$ , interacts at  $\mathbf{x}_{surf}$  with the time-varying sea surface  $S_f$  at time  $t_2$ . In state B, the material parameters inside the volume are identical to the ones in state A but here,  $S_f$  indicates only a hypothetical interface. Furthermore, the source and receiver positions have been interchanged and the time reversed. The pressure wavefield,  $p^B$ , that has interacted with the same sea surface as in state A, is propagated to the receivers  $\mathbf{x}_{sep}$  at the separation level  $S_0$  and is recorded at time  $t = t_1 - t_2$ , where  $t_1$  is the recording time for the scattered wavefield from the sea surface. Finally, the pressure gradient of the scattered wavefield is obtained after combining the wavefields from states A and B (see 2<sup>nd</sup> line of Eq. 1), where the pressure wavefield in state B has been converted to a pressure gradient wavefield,  $\nabla p^B$ .

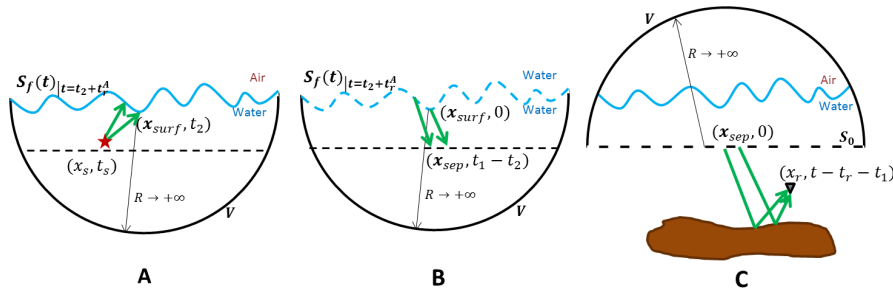


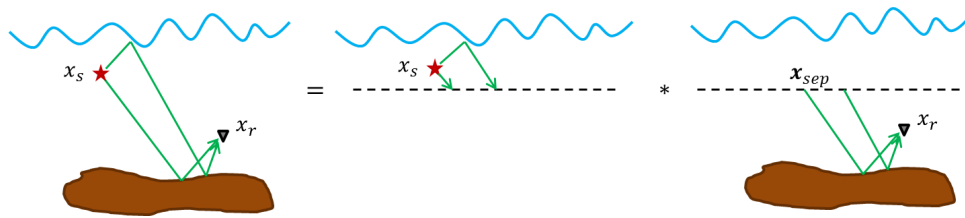
**Figure 1** Schematic depicting source ghost modelling by coupling wavefields from states A, B and C.

State C represents the subsurface reflectivity,  $p^{C^{-,+}}$ , that can be generated using any suitable modelling approach. The superscripts  $(-, +)$  indicate receiver side upgoing  $(-, \cdot)$  and source side downgoing  $(\cdot, +)$  wavefield components. In this equation,  $\mathbf{n}$  and  $\mathbf{n}_f$  are the outward-pointing unit normal vectors of the separation level and of the sea surface, respectively;  $t$  is the global time and  $t_r$  the recording time for the source ghost.

**Source deghosting:** Starting from the second line of Eq. 1 and adding the down-going direct wavefield from the source to the separation level, we denote the resulting wavefield as  $\nabla p^{SSR}$  (cf. Fig 2 middle) which is the pressure gradient of the direct wavefield with its ghost. Coupling this at the separation level  $S_0$  with the subsurface reflectivity,  $p^{C^{-,+}}$  (cf. Fig 2 right), we obtain the up-going primary wavefield with the source ghost,  $p_s^-$  (cf. Fig 2 left), as follow:

$$p_s^-(\mathbf{x}_r, t - t_r - t_s; \mathbf{x}_s, 0) = -2 \int_{-\infty}^{+\infty} \int_{S_0} [\nabla p^{SSR}(\mathbf{x}_{sep}, t_1; \mathbf{x}_s, t_s) p^{C^{-,+}}(\mathbf{x}_r, t - t_r - t_1; \mathbf{x}_{sep}, 0)] \cdot \mathbf{n} dS_0 dt_1 \quad (2)$$

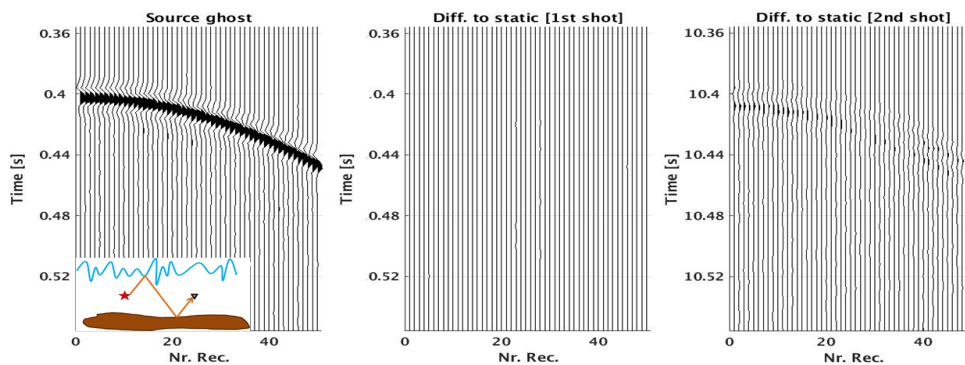
By inverting Eq. 2 in the frequency-space domain, one obtains the designated and deghosted primary wavefield,  $p^{C^{-,+}}$ .



**Figure 2** Sketch of the input data for the deghosting algorithm - the primary wavefield and its source ghost (left), the direct wavefield and its source ghost (middle) and subsurface reflectivity (right)

## Results

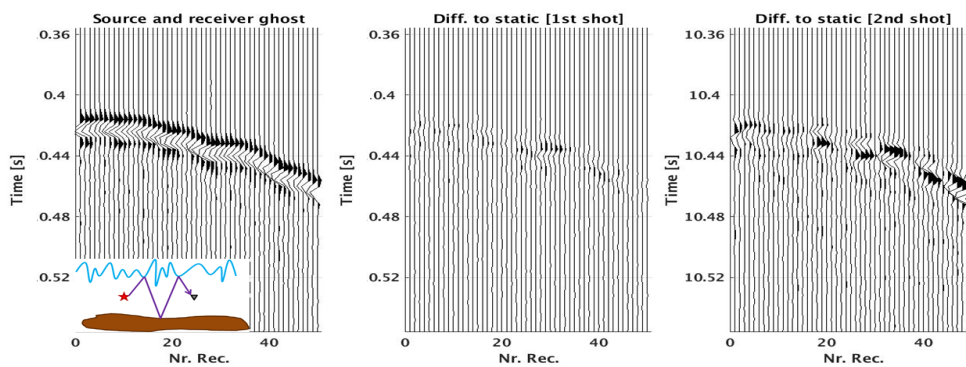
**Modelling:** Synthetic pressure data were created following Eq. 1. A time-varying sea surface was built from a Pierson-Moskowitz spectrum (wind-speed of 15m/s i.e. near gale, significant wave height of 4.8m and dominant wavelength of 203m). The subsurface reflection was generated from a flat reflector located at 300m depth. The source and receivers were placed at 15m depth. Figures 3-5 compare a shot gather from a frozen rough sea surface with shot gathers computed from a time-varying sea surface with sources fired at  $t = 0$ s (i.e. first shot) and  $t = 10$ s (i.e. second shot), respectively. The frozen rough sea surface corresponds to the sea surface shape at  $t = 0$ s for the time variant case.



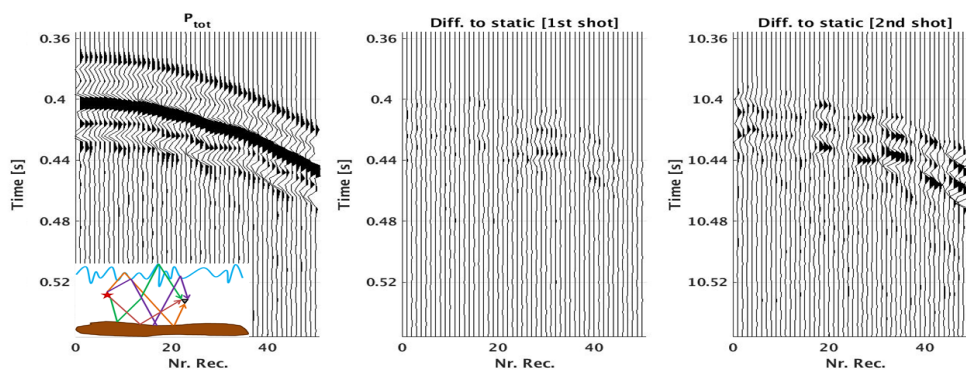
**Figure 3** Shot gather of the source ghost for a frozen rough sea surface (left panel), difference with the shot gather computed for a time-varying rough sea surface fired at time 0s (middle panel) and fired at time 10s (right panel).

Figure 3 represents the source ghost modeling while Figure 4 shows the source-receiver ghost modeling. Observe that in Figure 3 the differences between the first shot and the static case are small (cf. middle

panel). This is because only a short time has elapsed between the source firing and interacting with the sea surface, so the sea surface shape has not changed much. However, in comparison to the first shot, this difference has significantly increased in the second shot as expected (cf. Fig 3 right). In Figure 4, the wavefield has now interacted with the sea surface twice and thus allowed the sea surface shape to evolve in comparison to the static case. Hence the differences observed are quite significant for the first shot (cf. Fig 4 middle) and increased with the second shot (cf. Fig 4 right). Figure 5 includes all the ghost effects with the primary reflections and thus shows bigger differences since the receiver side ghost effects are also included, allowing the data to account for the time evolution of the sea surface. These results show that the interaction with a time-varying rough sea surface significantly affects the subsurface reflections. When data are acquired in rough weather conditions, such effects would make a significant contribution to 4D noise. Note that the receiver-side effects, evident in Figures 4 and 5, can be mitigated by use of a dual-sensor streamer. The complementary nature of the pressure and particle motion sensors allows the receiver-side ghost effects to be removed without requiring any knowledge of the nature of the sea surface. The remaining effects on the source side, shown in Figure 3, are still to be addressed but these are much smaller in magnitude in comparison to the receiver side.



**Figure 4** Shot gather of the source-receiver ghost for a frozen rough sea surface (left panel), difference with the shot gather computed for a time-varying rough sea surface fired at time 0s (middle panel) and fired at time 10s (right panel).



**Figure 5** Shot gather of the total pressure wavefield for a frozen rough sea surface (left panel), difference with the shot gather computed for a time-varying rough sea surface fired at time 0s (middle panel) and fired at time 10s (right panel).

**Deghosting:** The source deghosting algorithm for the time-varying rough sea surface is based on Eq. 2. To avoid instabilities in the inversion (arising from source ghost notches), the acquisition configuration is set up to consist of point sources at two complementary depth levels, 10 and 15m (Parkes and Hegna (2011)). The firing time of the shallower sources has also been randomized. The receivers are at 25m depth and we use the same time-varying sea surface as in the previous modelling case. The input data for the deghosting algorithm are the up-going pressure wavefield and the down-going direct wavefield with its source ghost recorded at the separation level. The required data can be obtained by applying wavefield separation to dual-sensor data. In Figure 6, we show the input up-going pressure wavefield

and the corresponding source deghosted and designatured result. Figure 6a represents the input data obtained using Eq.2 for the acquisition configuration described above. The data are displayed as receiver gathers for the central point at the separation level. Figure 6b is the receiver gather of the deghosted and designatured pressure wavefield resulting and Figure 6c displays the difference to the modeled subsurface reflectivity. Figures 6 (b and c) show wavefields computed at the separation level which explains the time shift compared to Figure 6a where the pressure wavefields have been computed at the source level. As highlighted in Figure 6c, the deghosting algorithm results match the modeled subsurface reflectivity very well.

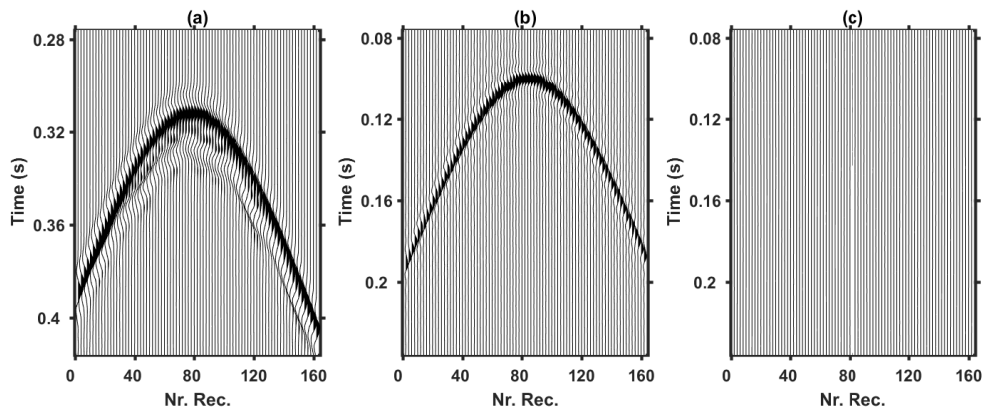


**Figure 6** Source designature and deghosting - (a) Up-going pressure wavefield obtained from Eq. 2, (b) deghosted and designatured pressure wavefield, and (c) difference to the modeled subsurface reflectivity.

## Conclusions

An algorithm based on acoustic reciprocity has been developed to model source ghosts for time-varying rough sea surfaces. Our modelling results highlight the fact that the interaction with time-varying sea surfaces affect the subsurface reflections which has significant implication for seismic repeatability. Consequently, accounting for the time-variation of rough sea surfaces in deghosting can be crucial for 4D studies. The effects are most significant on the receiver side, and these can be mitigated by dual-sensor acquisition.

## Acknowledgments

We thank PGS for permission to publish this work, and Anthony Day and Morten W. Pedersen for valuable discussions.

## References

- Amundsen, L. [2001] Elimination of free-surface related multiples without need of the source wavelet. *Geophysics*, **66**(1), 327–341.
- Asgedom, E., Orji, O., Klüver, T., Tabti, H. and Söllner, W. [2016] On Broadband Data and Rough Sea Surface Receiver Deghosting. In: *78th EAGE Conference and Exhibition 2016*.
- Ceconello, E., Asgedom, E., Orji, O. and Söllner, W. [2016] Modelling Seismic Data for Time-varying Rough Sea Surfaces. In: *78th EAGE Conference and Exhibition 2016*.
- Fokkema, J.T. and van den Berg, P.M. [1993] *Seismic applications of acoustic reciprocity*. Elsevier.
- Laws, R. and Kragh, E. [2002] Rough seas and time-lapse seismic. *Geophysical Prospecting*, **50**(2), 195–208.
- Orji, O.C., Söllner, W. and Gelius, L.J. [2012] Effects of time-varying sea surface in marine seismic data. *Geophysics*, **77**(3), P33–P43.
- Parkes, G. and Hegna, S. [2011] An acquisition system that extracts the earth response from seismic data. *First Break*, **29**(12).
- Tenghamn, R., Vaage, S., Borresen, C. et al. [2007] A dual-sensor, towed marine streamer; its viable implementation and initial results. In: *2007 SEG Annual Meeting*. Society of Exploration Geophysicists.